CEA/SACLAY
DSM

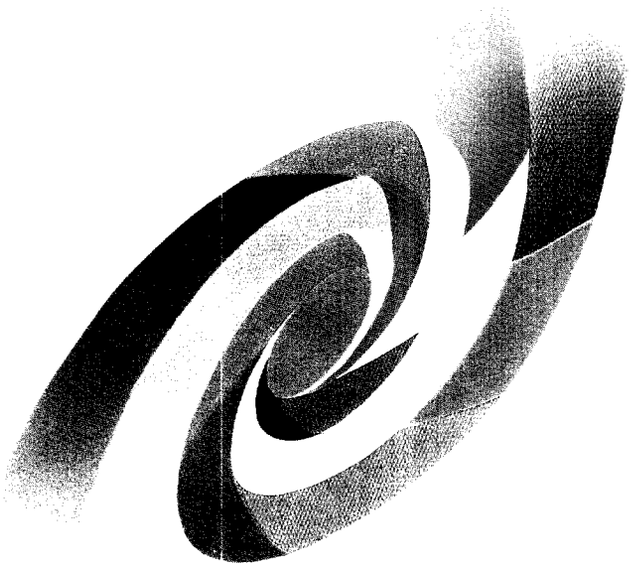

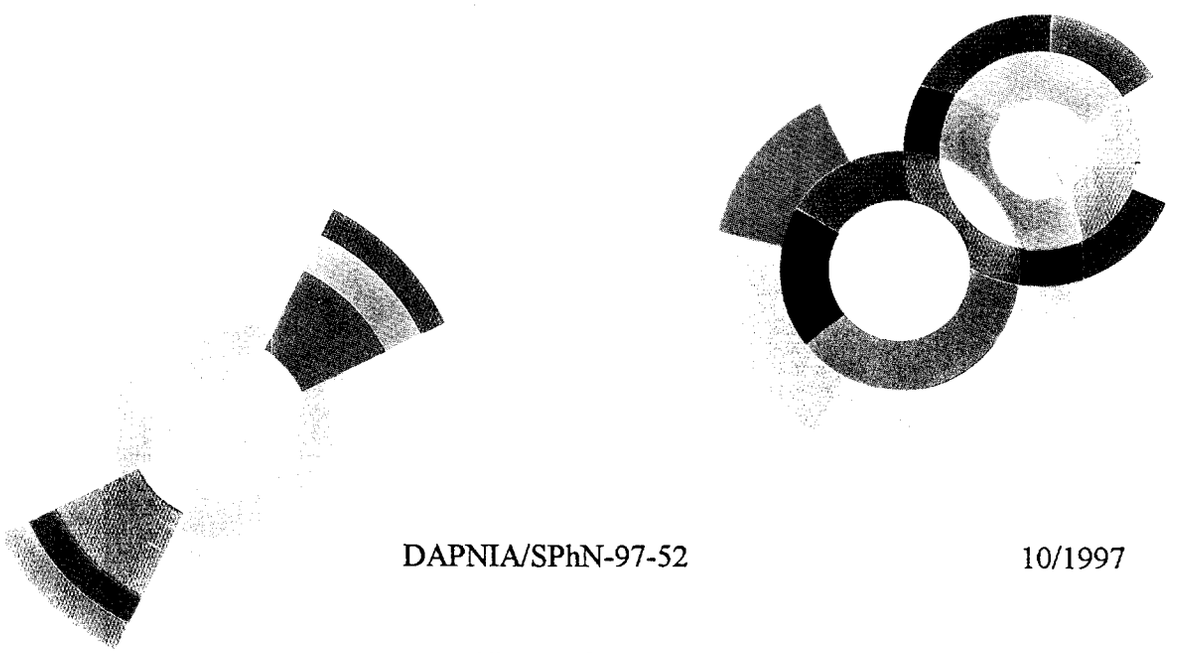

DAPNIA/SPhN-97-52 10/1997

Virtual Compton Scattering at the Nucleon

N. D'Hose, P. Bartsch, J. Berthot, P.Y. Bertin, V. Breton, W.U. Boeglin, R. Böhm, T. Caprano, S. Derber, N. Degrande, M. Distler, J.E. Ducret, R. Edelhoff, I. Ewald, H. Fonvieille, J. Friedrich, J.M. Friedrich, R. Geiges, Th. Gousset, P.A.M. Guichon, H. Holvoet, Ch. Hyde-Wright, P. Jennewein, M. Kahrau, S. Kerhoas, M. Korn, H. Kramer, K.W. Krygier, V. Kunde, B. Lannoy, D. Lhuillier, A. Liesenfeld, C. Marchand, D. Marchand, J. Martino, H. Merkel, K. Merle, P. Merle, G. De Meyer, J. Mougey, R. Neuhausen, E. Offermann, Th. Pospischil, G. Quemener, O. Ravel, Y. Roblin, J. Roche, G. Rosner, D. Ryckbosch, P. Sauer, H. Schmieden, S. Schardt, G. Tamas, M. Tytgat, M. Vanderhaeghen, L. Van Hoorebeke, R. Van de Vyver, J. Van de Wiele, P. Vernin, A. Wagner, Th. Walcher, S. Wolf.

DAPNIA

Département d'**A**strophysique, de Physique des **P**articules, de Physique **N**ucléaire et de l'**I**nstrumentation **A**ssociée
CEA/Saclay F-91191 Gif-sur-Yvette Cédex

VIRTUAL COMPTON SCATTERING ON THE NUCLEON

N. d'Hose[a], P. Bartsch[d], J. Berthot[b], P.Y. Bertin[b], V. Breton[b], W.U. Boeglin[g], R. Böhm[d], T. Caprano[d], S. Derber[d], N. Degrande[c], M. Distler[d], J.E. Ducret[a], R. Edelhoff[d], I. Ewald[d], H. Fonvieille[b], J. Friedrich[d], J.M. Friedrich[d], R. Geiges[d], Th. Gousset[a], P.A.M. Guichon[a], H.Holvoet[c], Ch. Hyde-Wright[e], P. Jennewein[d], M. Kahrau[d], S. Kerhoas[a], M. Korn[d], H. Kramer[d], K.W. Krygier[d], V. Kunde[d], B.Lannoy[c], D. Lhuillier[a], A. Liesenfeld[d], C. Marchand[a], D. Marchand[a], J. Martino[a], H. Merkel[d], K. Merle[d], P. Merle[d], G. De Meyer[c], J. Mougey[a], R. Neuhausen[d], E. Offermann[f], Th. Pospischil[d], G. Quemener[b], O. Ravel[b], Y. Roblin[b], J. Roche[a], G. Rosner[d], D. Ryckbosch[c], P. Sauer[d], H. Schmieden[d], S. Schardt[d], G. Tamas[d], M. Tytgat[c], M. Vanderhaeghen[a], L. Van Hoorebeke[c], R. Van de Vyver[c], J. Van de Wiele[h], P. Vernin[a], A. Wagner[d], Th. Walcher[d], S. Wolf[d].

[a] *CEA DAPNIA-SPhN, C.E. Saclay, France*
[b] *LPC, Univ. Blaise Pascal, IN2P3 Aubiere, France*
[c] *University of Gent, Belgium*
[d] *Institut für Kernphysik, Universität Mainz, Germany*
[e] *Old Dominium University, Virginia, U.S.A*
[f] *C.E.B.A.F, Virginia, U.S.A*
[g] *Florida International University, Miami,Florida, U.S.A*
[h] *IPN, IN2P3 Orsay, France*

The Virtual Compton Scattering allows us to measure for the first time the generalized polarizabilities of the proton. The experimental method used to extract these new observables is presented as well as some preliminary results obtained at MAMI.

Virtual Compton Scattering is a fundamental exclusive reaction off the proton which provides us with a new insight of the internal structure of the nucleon. Below π^0 production threshold ($M_p < \sqrt{s} < M_p + M_\pi$, but arbitrary Q^2), this experiment measures the generalized polarizabilities of the proton [1]. They are fundamental electromagnetic observables of the nucleon, functions of Q^2, and are complementary to the elastic form factors. At $Q^2 = 0$ with real photons, we get the usual electric (α) and magnetic (β) polarizabilities. In the energy domain provided at MIT-Bates [2], MAMI [3] and CEBAF [4], these observables will be measured at $Q^2 = 0.05$, 0.33, 1. to 3. GeV^2 respectively. The experimental method used to extract these new observables is presented in this paper as well as some preliminary results obtained at MAMI.

1 Concept of Polarizabilities

The idea behind the concept of electromagnetic polarizabilities can be easily understood by a comparison with classical physics. If we consider an electron (of charge $-e$ and mass m_e) moving inside a sphere of radius a and total charge $+e$ uniformly distributed (atomic Thomson model), the local electric field acting on the electron is :

$$\vec{E}_{local} = \frac{e}{4\pi\epsilon_0}\frac{\vec{r}}{a^3} = \frac{m_e\omega_o^2}{e}\vec{r} \tag{1}$$

The electron is constrained by a spring strength (of constant ω_0). If an external electric field $\vec{E_{ext}} = \vec{E}_o e^{-i\omega t}$ polarizes the system, an electric dipole moment $\vec{d}$ is induced :

$$\vec{d} = -e\vec{r} \equiv \alpha\vec{E}_{ext}, \tag{2}$$

where α is defined as the polarizability. The dynamical equation applied to the electron gives :

$$\alpha = \frac{e^2}{m_e}\frac{1}{(\omega_0^2 - \omega^2)} \overset{\omega\to 0}{\to} 4\pi\epsilon_0 a^3 \tag{3}$$

The denominator of the general formula indicates clearly that the polarizability determines the stiffness of the system which is related to its internal structure. We note easily that the dimension of the polarizability in this case is a volume.

The radiative power of this system, denoted $P_{Rayleigh}$, is given by the antenna formula and can be related to the electromagnetic energy density u_{em} and the Rayleigh cross section :

$$P_{Rayleigh} = \frac{<\ddot{\vec{d}}>^2}{6\pi\epsilon_0 c^3} = u_{em} \times c \times \sigma_{Rayleigh} \tag{4}$$

$$\sigma_{Rayleigh} = \frac{\alpha^2}{6\pi\epsilon_0^2 c^4}\omega^4 = \sigma_{Thomson}\frac{\omega^4}{(\omega_o^2 - \omega^2)^2} \tag{5}$$

where $\sigma_{Thomson} = \frac{8\pi}{3}r_0^2$ is obtained for the free electrons ($\omega_0 = 0$) and $r_0 = \alpha_{QED}/m_e$ is the classical radius of the electron.[a] The Rayleigh scattering is proportional to α^2 and ω^4, which implies the well-known phenomena of blue skies and red sunsets.

[a] In this classical calculation, we use the MKSA unity system where $\alpha_{QED} = e^2/4\pi\epsilon_0\hbar c$. In the Real Compton Scattering, the theory of which has been known for several decades, we use the Gauss unity system : $\alpha_{QED} = e^2$. In the Virtual Compton Scattering, developed more recently, we use the Heaviside unity system : $\alpha_{QED} = e^2/4\pi$.

We can have also a more complete picture of the polarizability in quantum mechanical expression. Let us consider a system which eigenstates are noted $|0>, ...|N>$ with eigen energies $E_0, ...E_N$. If we apply a perturbation W with an external electric field parallel to the z direction, $W = -\vec{d}.\vec{E}_{ext} = -d_z E_{ext}$. The new eigenstates can be evaluated at the first order of the perturbation with :

$$|0'>=|0> - \sum_{N\neq 0} \frac{<N|W|0>}{E_N - E_0}|N> + O(W^2) \quad (6)$$

An electric dipole moment $\vec{d}$ is induced : $<\vec{d}>= \alpha \vec{E_{ext}}$

$$<d_z>=<0'|d_z|0'>=<0|d_z|0> + 2E_{ext} \sum_{N\neq 0} \frac{|<N|d_z|0>|^2}{E_N - E_0} + ... \quad (7)$$

For a symmetrical system, the first term is zero, so the polarizability has the general formula :

$$\alpha = 2 \sum_{N\neq 0} \frac{|<N|d_z|0>|^2}{E_N - E_0} \quad (8)$$

This formula has the same form as the previous expression obtained using classical mechanics if we multiply both the numerator and denominator by r^2. It has the extra advantage that it shows clearly that we are sensitive to the whole excitation spectrum of the system. Below π^0 production threshold, the excited states contribute virtually. This is an advantage over real resonance production for which meson production and rescattering are the dominant process and must be treated explicitly even though they are not the interesting part of the problem in so far as nucleon structure is concerned. Below the pion production threshold, the situation is simpler because the excited states cannot decay and therefore have no width, which is the hypothesis of most theoretical models of nucleon structure. This advantage is similar to the Deep Inelastic Scattering regime for which it makes sense to use the parton model because the partons fragmentation can be neglected.

2 Real Compton Scattering

Let us consider Compton scattering off a nucleon of charge e and mass m. Let $\vec{q}$ and $\vec{\epsilon}$ be the momentum and polarization vectors of the incoming photon, q' and $\vec{\epsilon'}$ the corresponding ones for the scattered photon at an angle θ in the Laboratory frame. The photon energies are $\nu = |\vec{q}|$ and $\nu' = |\vec{q'}|$ respectively

where $\nu' = \nu/(1 + \frac{\nu}{m}(1 - cos\theta))$. The non polarized amplitude for low-energy Compton scattering when expanded to second order in ν is [5,6] :

$$T(\gamma N \to \gamma N) = -\left(\frac{e^2}{m} - \frac{e^2 < r^2 >}{6m}(\vec{q}^2 + \vec{q'}^2) + \alpha\nu\nu'\right)\vec{\epsilon}\vec{\epsilon'} + \beta(\vec{\epsilon}\wedge\vec{q})(\vec{\epsilon'}\wedge\vec{q'}) + 0(\nu^3) \tag{9}$$

We recognize first the constant Thomson term and then a modified Rayleigh term. The differential cross section as a function of the scattering angle is :

$$\frac{d\sigma}{d\nu} = \frac{d\sigma_{point}}{d\nu} - \frac{e^2}{m}\left[\frac{\nu'}{\nu}\right]^2 \nu\nu'\left[\frac{\bar{\alpha} + \bar{\beta}}{2}(1 + cos\theta)^2 + \frac{\bar{\alpha} - \bar{\beta}}{2}(1 - cos\theta)^2\right] + 0(\nu^4) \tag{10}$$

where $d\sigma_{point}/d\nu$ is the Powell cross section, the one for the Compton Scattering on a pointlike nucleon (with charge, spin and also anomalous magnetic moment). The Compton scattering polarizabilities $\bar{\alpha}$ and $\bar{\beta}$ are not equal to the static ones [5,6].

$$\bar{\alpha} = 2e^2 \sum_{N \neq 0} \frac{|< N|d_z|0 >|^2}{E_N - E_0} + \frac{e^2 < r^2 >}{3m} \tag{11}$$

$$\bar{\beta} = 2e^2 \sum_{N \neq 0} \frac{|< N|\mu_z|0 >|^2}{E_N - E_0} - \frac{e^2 < r^2 >}{6m} - \frac{e^2 < d^2 >}{2m} \tag{12}$$

$\bar{\alpha}$ and α differ by a positive correction factor which is due to the finite size or retardation effect. For the magnetic polarizability the corrections are more subtle. We have two negative (diamagnetic) contributions : one is due to a counterpart in the retardation effect, the other is due to the seagull term.

A recent paper [7] of MacGibbon *et al.* refers all the experiments which have been carried out since twenty years ago and provides the global average $\bar{\alpha} = (12.1 \pm 0.8 \pm 0.5)10^{-4}$ fm^3 and $\bar{\beta} = (2.1 \mp 0.8 \mp 0.5)10^{-4}$ fm^3 where the first error is the combined statistical and systematic error propagated from the individual cross sections and the second is a model-dependent error.

Non-Relativistic Constituent Quark Model which was developed by Isgur and Karl [8] provides a simple calculation of the value of the polarizabities. This model has essentially three parameters. The basic degrees of freedom are massive constituent quarks (of mass $m \simeq 0.34$ GeV) moving within a harmonic oscillator confining potential and additional hyperfine interactions. The oscillator parameter can be estimated from the masses of the lowest negative parity (p-shell) N^* resonances as compared to the average mass of the nucleon and the $\Delta(1232)$ (s-shell) ($\hbar\omega \simeq 500$ MeV and then $< r^2 >= m\omega^{-1}$). The electric and magnetic polarizabilities are governed by the $N \to N^*$ and $N \to \Delta$

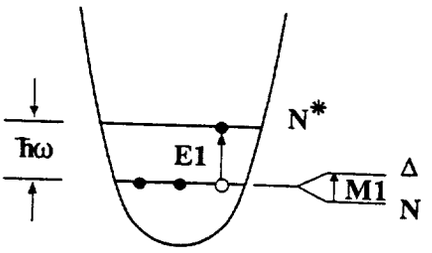

Figure 1: Electric and magnetic dipole interactions in a naive oscillator quark model.

transitions respectively, as illustrated in Fig. 1. In this model, the value of the magnetic polarizability is too high, while the electric polarizability is really too small.

One of the limitations of the Non-Relativistic Constituent Quark Model is that it has no relationship to chiral symmetry, an important property of QCD which governs much of low energy hadron physics. Chiral symmetry is spontaneously broken ; the pion is the corresponding Goldstone boson. Chiral perturbation theory predicts better results for the two polarizabilities[9]. This implies that the polarizabilities are clearly related to the pion cloud. It is then really important to see the transition from pion degrees of freedom to quarks, with the evolution of the polarizabilities as a function of Q^2.

3 Virtual Compton Scattering

This exclusive reaction $ep \rightarrow e'p'\gamma'$ is defined by five kinematical independent variables : ϵ, Q^2, s, (these three ones depend only on the electron kinematics), $\theta_{\gamma\gamma}$ (noted also for convenience θ) (angle between the two photons) and ϕ (azimuthal angle of the electron plane with respect to the hadron plane). Since we are in a kinematical regime defined by a center of mass (CM) energy $\sqrt{s}$ of the final proton-photon system close to threshold and below pion photoproduction threshold, it is natural to work in the CM frame and to use q and q' the modulus of the momentum of the real and virtual photon respectively, instead of Q^2 and s. The relations between these two sets of variables are $q' = (s - m^2)/2\sqrt{s}$ and $q = (Q^2 + (s - Q^2 - m^2)^2/4s)^{\frac{1}{2}}$; q' varies from 0 to ~125 MeV.

The cross section has the form :

$$\frac{d^5\sigma}{dk'_{lab}[d\Omega_e]_{lab}[d\Omega_p]_{CM}} = \frac{(2\pi)^{-5}}{64m}\left(\frac{k'_{lab}}{k_{lab}}\right)\frac{s-m^2}{s} \times \mathcal{M}^{exp} \qquad (13)$$

where $\mathcal{M}^{exp}$ is invariant under a Lorentz transformation.

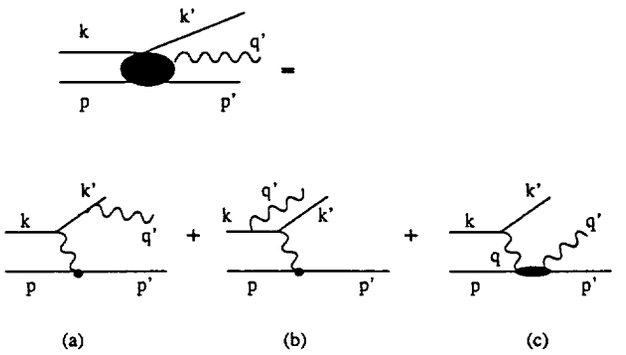

Figure 2: The $p(e,e'p)\gamma$ reaction. The initial, final electron and initial, final proton quadri-momenta are k, k' and p, p' respectively. The final photon quadri-momentum is q'. In the one photon exchange approximation, a) and b) correspond to the Bethe-Heiler (BH) process. c) corresponds to the Full Virtual Compton Scattering (FVCS) process. We note q the quadri-momentum of the virtual photon exchanged in the VCS process, that is $q = k - k'$.

In this reaction, the final photon can be emitted either by the electron or by the proton (see Fig. 2). The first process is described by Bethe-Heitler (BH) amplitude which is calculable from Quantum Electro-Dynamics (QED) (if the proton form factor are well known). The second process is described by the Virtual Compton Scattering (VCS) amplitude that can be split in two parts : the Born term containing only the nucleon and anti-nucleon contributions (exactlly calculable) and the Non-Born term related to the excited states. The probability $\mathcal{M}^{exp}$ (which is the differential cross section divided by a phase space factor) is therefore a coherent sum of the different amplitudes,

$$\mathcal{M}^{exp} = \frac{1}{4}\sum_{spin} |T^{BH} + T^{VCS}|^2 = \frac{1}{4}\sum_{spin} |T^{BH} + T^{Born} + T^{NonBorn}|^2 \quad (14)$$

The low energy theorem from Low[10] says that in an expansion in powers of the outgoing photon energy (q') in the final photon-proton center of mass system, the first term of the amplitudes T^{BH} and T^{Born} is of the order q'^{-1}, while the first term of $T^{NonBorn}$ is of the order q'^{1}. Then the two first terms of the probability $\mathcal{M}^{exp}$, of the order q'^{-2} and q'^{-1} are only due to the interference of the BH and Born amplitudes and are completely calculable. The effect of the nucleon structure appears from the q'^{0} term. The leading order of the Non-Born amplitude is parametrized by Guichon *et al.*[1] with 10 generalized

polarizabilities (GPs) as functions of the initial photon momentum q. They are noted $P^{(\rho' L', \rho L) S}$ or $\hat{P}^{(\rho' L', L) S}$, where $L(L')$ denotes the initial (final) photon orbital angular momentum, $\rho(\rho')$ the type of multipole transition [$0 = C$ (scalar, Coulomb), $1 = M$ (magnetic), $2 = E$ (electric)], and S distinguishes between non-spin-flip ($S = 0$) and spin-flip ($S = 1$) transitions. Selection rules based on parity and angular momentum conservation give only ten GPs, three scalar ones, $P^{(01,01)0}$ ($\stackrel{\mathrm{q}\to 0}{\to} -\sqrt{2/3}\ \alpha/e^2$), $P^{(11,11)0}$ ($\stackrel{\mathrm{q}\to 0}{\to} -\sqrt{8/3}\ \beta/e^2$), $\hat{P}^{(01,1)0}$ and seven vector ones, $P^{(01,01)1}$, $P^{(01,12)1}$, $\hat{P}^{(01,1)1}$, $P^{(11,11)1}$, $P^{(11,00)1}$, $P^{(11,02)1}$, $\hat{P}^{(11,2)1}$. Recently, it has been proved by Drechsel *et al.* [11] that only six of the above ten GPs are independent, if one requires combined crossing and charge-conjugation symmetries to hold. For example :

$$-\frac{3\mathrm{q}^2}{2\tilde{q}_0}\hat{P}^{(01,1)0}(\mathrm{q}) = \sqrt{3/2}P^{(01,01)0}(\mathrm{q}) + \sqrt{3/8}P^{(11,11)0}(\mathrm{q}) \qquad (15)$$

where $\tilde{q}_0 = m - \sqrt{m^2 + \mathrm{q}^2}$ is the virtual photon center of mass energy when $\mathrm{q}' = 0$. According to reference [1], the experiment near threshold ($\mathrm{q}' \leq m_\pi$) has to determine $\mathcal{M}^{exp}$ in the form :

$$\mathcal{M}^{exp} = \frac{\mathcal{M}^{exp}_{-2}}{\mathrm{q}'^2} + \frac{\mathcal{M}^{exp}_{-1}}{\mathrm{q}'} + \mathcal{M}^{exp}_0 + 0(\mathrm{q}') \qquad (16)$$

where the coefficients $\mathcal{M}^{exp}_i$, i=-2,-1,0 are functions of $(\mathrm{q}, \epsilon, \theta, \varphi)$. The experimental method (see Fig. 3) is to study the evolution of $\mathrm{q}'^2\mathcal{M}^{exp}$ at small values of q'. The ordinate and slope at $\mathrm{q}' = 0$ are due only to the interference between BH and Born and their experimental values have to be in perfect agreement with the low energy theorem predictions (LET). This is a crucial part of the experiment because it validates the following step which is the extraction of some GPs from the next order of the expansion. In fact with an unpolarized experiment, the difference $\mathcal{M}^{exp}_0 - \mathcal{M}^{LET}_0$ provides some linear combinations of GPs :

$$\mathcal{M}^{exp}_0 - \mathcal{M}^{LET}_0 = \frac{4me^6\mathrm{q}}{\tilde{Q}^2(1-\epsilon)}\sqrt{\frac{2\sqrt{\mathrm{q}^2+m^2}}{\sqrt{\mathrm{q}^2+m^2}+m}} \qquad (17)$$

$$\{sin\theta\,(\omega'' sin\theta - \omega' \mathrm{k_T} cos\varphi cos\theta)\,(\epsilon P_{LL}(\mathrm{q}) - P_{TT}(\mathrm{q}))$$

$$-\,(\omega'' sin\theta cos\varphi - \omega' \mathrm{k_T} cos\theta)\,\sqrt{2\epsilon(1+\epsilon)}P_{LT}(\mathrm{q})$$

$$-\,\left(\omega'' sin\theta cos\theta cos\varphi - \omega' \mathrm{k_T}(1 - cos^2\varphi sin^2\theta)\right)\sqrt{2\epsilon(1+\epsilon)}P'_{LT}(\mathrm{q})\Big\}$$

where the various kinematic coefficients are : $\tilde{Q} = [Q]_{q'=0}$

$$\omega = -\left[q'\left(\frac{1}{p.q'} + \frac{1}{k.q'}\right)\right]_{q'=0} \; ; \; \omega' = +\left[q'\left(\frac{1}{k'.q'} - \frac{1}{k.q'}\right)\right]_{q'=0} \tag{18}$$

$$k_T = \tilde{Q}\sqrt{\frac{\epsilon}{2(1-\epsilon)}} \; ; \; \omega'' = +\left[\omega q - \omega'\sqrt{k'^2 - k_T{}^2}\right]_{q'=0}$$

The amplitudes $P_{LL}(q), P_{TT}(q), P_{LT}(q)$ and $P'_{LT}(q)$ are the following combination of generalized polarizabilities (where G_E and G_M are the form factors applied at $\tilde{Q}^2$) :

$$P_{LL} = -2\sqrt{6}mG_E P^{(01,01)0}(q) \tag{19}$$

$$P_{TT} = \tfrac{3}{2}G_M\left(2\tilde{q}_0 P^{(01,01)1}(q) + \sqrt{2}q^2(\sqrt{3}\hat{P}^{(01,1)1}(q) + P^{(01,12)1}(q)\right)$$

$$P_{LT} = \sqrt{\tfrac{3}{2}}m\frac{q}{\tilde{Q}}G_E P^{(11,11)0}(q) + \frac{\sqrt{3}\tilde{Q}}{2q}G_M\left(P^{(11,00)1}(q) + \frac{q^2}{\sqrt{2}}P^{(11,02)1}(q)\right)$$

$$P'_{LT} = \sqrt{\tfrac{3}{2}}\frac{m}{\tilde{Q}}G_E\left(2\tilde{q}_0 P^{(01,01)0}(q) + \sqrt{6}q^2\hat{P}^{(01,1)0}(q)\right) - \tfrac{3}{2}\tilde{Q}G_M P^{(01,01)1}(q)$$

With the crossing and charge-conjugation symmetries, the two last combinations are related by the relation :

$$P'_{LT}(q) = -\frac{\tilde{q}_0}{q}P_{LT}(q) \tag{20}$$

In order to extract $\epsilon P_{LL} - P_{TT}$ and P_{LT} we have to play with different sets (θ, φ). Figure 5 shows the dominant contribution of the Bethe-Heitler amplitude in the direction of the incident or outgoing electron, a significant effect of the polarizabilities can be measured only far from the electron lines. The equations (17-19) show that an experiment performed at $\theta = 0$ (whatever φ) will provide directly P_{LT} (mainly related to the polarizability $P^{(11,11)0}$). To separate P_{LL} (or $P^{(01,01)0}$) from P_{TT} we need at least two values of ϵ.

Several predictions exist in order to evaluate the effects of the GPs :

- Guichon, Liu, and Thomas[1] made a first estimate of generalized polarizabilities in a non relativistic quark model (NRQCM) in order to guide the first generation of experiments. In this model, only seven of the ten generalized polarizabilities are non zero. In a later publication, Liu, Thomas and Guichon [12]extented their calculation to include recoil effects.

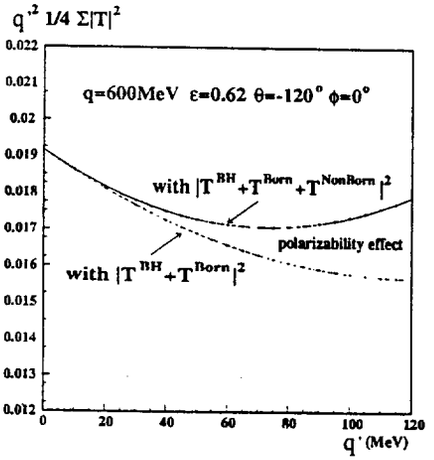

Figure 3: Evolution of $q'^2 \times \mathcal{M}^{exp}$ from calculations of M. Vanderhaeghen. The ordinate and slope at $q' = 0$ are due only to the interference between BH and Born, while the polarizability effect appears in the second order of the expansion.

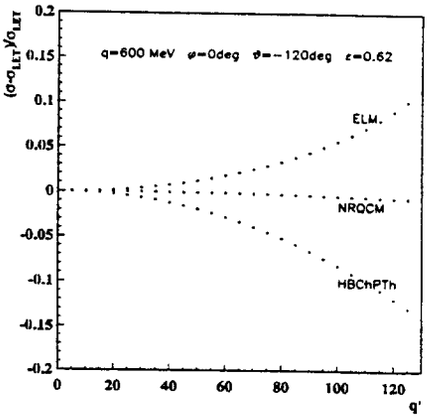

Figure 4: Deviation from LET predictions in three models described in the paper.The deviation takes into account all the orders of the expansion in $q' = 0$ for the NonBorn amplitude in ELM, and only the first order for NRQCM and HBCHPT.

- Vanderhaeghen [13] performed a calculation in an effective Lagrangian approach (ELM) including nucleon resonance effects. The polarization of the pion cloud is also taken into account by direct coupling of the photon to the pion or pion pair.

- Metz and Drechsel [14] performed a one-loop calculation of the polarizabilities in the linear sigma model (LSM) in the limit of an infinite sigma mass.

- A calculation in the heavy-baryon chiral perturbation theory (HBChPT) has also been performed to third order in the initial and final photon momentum expansion by Hemmert, Holstein, Knöchlein and Scherer [15]. The range in momentum transfer over which this expansion is valid is limited by the order to which the expansion is carried. This calculation is expected to work up a momentum transfer of q = 300 MeV.

The expected deviation at the MAMI kinematics from the LET :

$$(\sigma_{BH+Born+NonBorn} - \sigma_{BH+Born})/\sigma_{BH+Born}$$

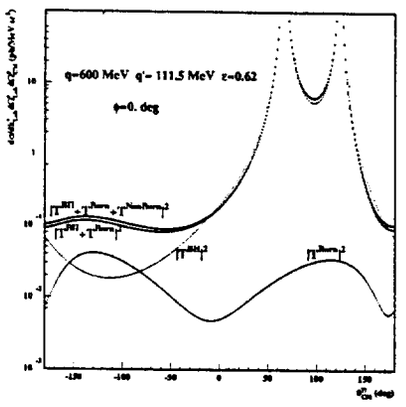

Figure 5: The contributions $|T^{BH}|^2$, $|T^{Born}|^2$, $|T^{BH} + T^{Born}|^2$, $|T^{BH} + T^{Born} + T^{NonBorn}|^2$ are indicated in a logarithmic scale in the kinematical domain studied at MAMI. The "generalized" polarizabilities introduced in the Non Born term are estimated in the ELM.

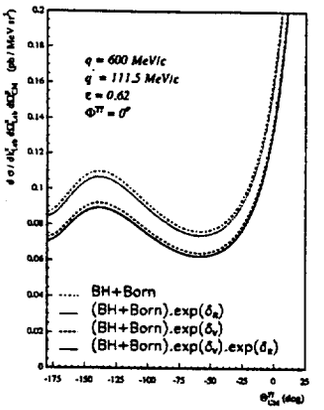

Figure 6: Effect of the real and virtual radiative corrections on the total BH+Born cross section according the calculation of M. Vanderhaeghen *et al.*.

is reported in Fig. 4 in the framework of the three models NRQCM, ELM, HBChPT (though for the latter q = 600 MeV might be too large). The effect is of the order of 10% and is positive only in the ELM. It is important to note that in the ELM, the complete calculation for the Non Born amplitude (with all the orders of the expansion in q') is carried out. For the two other models only the prediction of the GPs is available, and the deviation is evaluated using the formula (17-19), that is the first order of the expansion.

4 Preliminary results at MAMI

The experiment is performed in the A1 Hall at MAMI. The scattered proton and electron are detected in coincidence in two magnetic spectrometers and the final photon is tagged by the reconstructed missing mass: $M_X^2 = 0$. With the high duty cycle available at MAMI, one is not limited by the accidental counting rates and one can use a typical luminosity of $\mathcal{L} = 2.10^{37}\ \mathrm{cm}^{-2}\mathrm{s}^{-1}$. Thanks to the excellent resolution of the facilities ($\Delta E/E = 10^{-4}$ for the energy of the incident electrons, $\Delta P/P = 10^{-4}$ for the momenta of the two spectrometers

and an angular resolution better than 3 mrad) the contribution of the π^0 in the missing mass is very clearly separated from the events characterized by the photon mass (see Fig. 7).

The radiative corrections have been calculated for the first time by Vanderhaeghen *el al.* taking into account all the diagrams of order α^4 in the cross section [16]. The dimensional regularization scheme to treat both Ultra-Violet and Infra-Red divergences is used. The expression of the virtual photon correction contains analytical terms and a numerical term which has been computed. The real photon correction is splitted in two parts, one which depends on the cut in missing mass and the other one which depends on the electron kinematics (electron angle, velocity, and Q^2). After exponentiation of the radiative corrections, one gets -16% for the virtual one, and -3% for the real one as shown in Fig. 6. Continuity between the radiative corrections in the elastic case and the VCS case has been checked.

Figure 8 shows preliminary results obtained at q' = 45 MeV. Data points are corrected for radiative effects. The two sets of black and squared points are obtained at two different periods, and the triangle points are obtained at a different position for the proton spectrometer. They are in rather good agreement in the region of same kinematics. The LET prediction is also indicated by the curve. As q' is small, the deviation from the LET prediction has to be very small (see Fig. 4) and these data provide first test of the low energy theorem for VCS. This represents a severe check of our analysis method and of the radiative corrections. It will ensure a reliable extraction of the polarizabilities in the energy domain q'=100 MeV. This is necessary to have a very good control of the absolute value of the experimental cross section, in order to measure the expected small deviation from the LET prediction.

Polarizabilities are very clean observables to access the internal structure of the nucleon, but it is a long way to get these observables, as we need to perform absolute measurements with a very great precision.

References

1. P.A.M. Guichon, G. Liu, A.W. Thomas, *Nucl. Phys.* A **591**, 606 (1995)
2. B. Asavapibhop *et al.* , proposal at Bates (1997)
3. N. d'Hose *et al.* , proposal at MAMI (1995)
4. G. Audit *et al.* , CEBAF proposal PR 93-050 (1993)
5. W. Weise, Baryon Spectroscopy and the Structure of the Nucleon, International Workshop at Saclay, edited by H.P. Morsch and M. Soyeur (1991)
6. B. König, D. Drechsel, L. Tiator, Perspectives on Photon Interactions

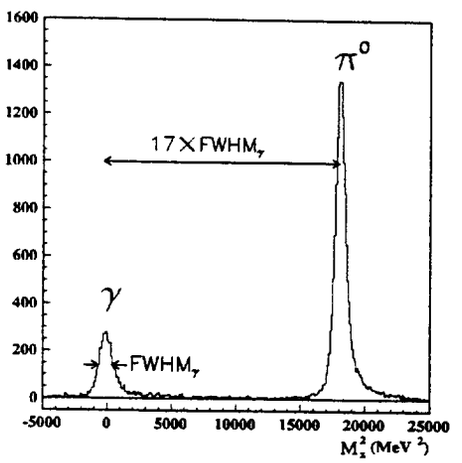

Figure 7: Experimental spectrum of the missing mass in the reaction p(e,e'p)X with a very good separation between Compton and π^0 electroproduction events.

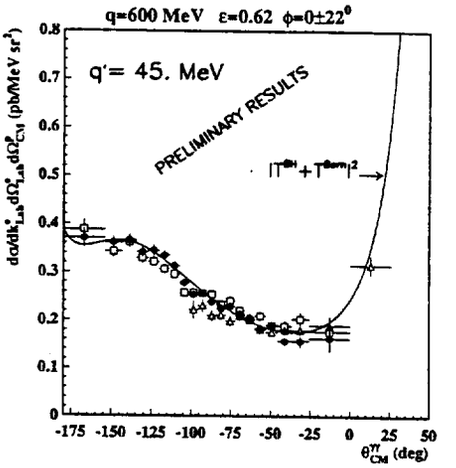

Figure 8: Preliminary results at q'=45 MeV. Different sets of data are reported. The curve presents the low energy theorem prediction.

with Hadrons and Nuclei, Lecture Notes in Physics, Vol. 365, edited by M. schumacher and G. Tamas (1990)

7. B.E. MacGibbon *et al.* , *Phys. Rev.* C **52**, 2097 (1995)
8. N. Isgur and G. Karl, *Phys. Rev.* D **18**, 4187 (1978), *Phys. Rev.* D **19**, 2653 (1979)
9. V. Bernard, N. Kaiser, U.-G. Meissner, and A. Scmidt, *Phys. Lett.* B **319**, 269 (1993), *Z. Phys.* A **348**, 317 (1994), T.R. Hemmert, B.R. Holstein and J. Kambor, *Phys. Rev.* D **55**, 5598 (1997)
10. F.E. Low, *Phys. Rev.* **96**, 1428 (1954)
11. D. Drechsel, G. Knöchlein, A. Metz, and S. Scherer, *Phys. Rev.* C **55**, 424 (1997), Mainz Report No. nucl-th/9705010
12. G.Q. LIU, A.W. THOMAS AND P.A.M. GUICHON, Aust. J. Phys. **49** (1996) 905
13. M. Vanderhaeghen, *Phys. Lett.* B **368**, 13 (1996)
14. A. Metz and D. Drechsel, Mainz Report No. MKPH-T-96-17
15. T.R. Hemmert, B.R. Holstein, G. Knöchlein and S. Scherer, *Phys. Rev.* D **55**, 2630 (1997), *Phys. Rev. Lett.* **79**, 22 (1997)
16. M. Vanderhaeghen, D. Lhuillier, D. Marchand and J. Van de Wiele, to be published